Available online at www.sciencedirect.com
ScienceDirect
Journal of the European Ceramic Society 31 (2011) 931–940
www.elsevier.com/locate/jeurceramsoc

Synthesis and structural characterization of SiBOC ceramic fibers derived from single-source polyborosiloxane

H.W. Bai [a], G. Wen [a,b,*], X.X. Huang [a], Z.X. Han [a], B. Zhong [a], Z.X. Hu [a], X.D. Zhang [a]

[a] School of Materials Science and Engineering, Harbin Institute of Technology, Harbin 150001, PR China
[b] School of Materials Science and Engineering, Harbin Institute of Technology (Weihai), Weihai 264209, PR China

Received 15 June 2010; received in revised form 7 November 2010; accepted 24 November 2010
Available online 14 December 2010

Abstract

SiBOC ceramic fibers have been successfully prepared from single-source polyborosiloxanes which are synthesized from polymethylethoxysiloxane and $B(OH)_3$ via a sol–gel route. The morphological change, structural evolution and crystallization behavior of fibers as a function of thermal treatment are studied by several techniques. Polyborosiloxane sols exhibit remarkable spinnability, in which B atoms are homogenously incorporated into the linear Si–O–Si skeleton via Si–O–B bridges. SiBOC ceramic fibers with diameters of about 10 μm are prepared with high ceramic yield ranging from 80.5 to 86%. Although a continuous structural evolution occurs with increasing pyrolysis temperature, the SiBOC ceramic fiber with B/Si atom ratio of 0.14 is thermal stable at 1500 °C. The thermolysis and crystallization behaviors are closely related to the boron content. The tendency toward crystallization of SiC and graphitization of free carbon is strengthened with the increase of boron content and pyrolysis temperature.
© 2010 Elsevier Ltd. All rights reserved.

Keywords: Fibers; Sol–gel processes; SiBOC fibers; Thermal properties; Microstructure-final

1. Introduction

Ceramic fibers are attractive choices for reinforcing ceramic matrix composite materials[1] owing to excellent properties such as thermal stability, high-temperature mechanical properties. Silicon oxycarbide (SiOC) glasses have received great deal of attention due to their enhanced chemical, mechanical and thermal properties compared with pure silica.[2–4] It is believed that the enhancement is attributed to the incorporation of carbon into silicate glasses which strengthens the molecular structure. SiOC fibers have been fabricated by sol–gel method and polymer-derived ceramic route.[5,6] However, the high-temperature decomposition of SiOC glasses, which occurs at temperature above 1350 °C due to carbothermal reduction between silica and carbon,[7] results in significant weight loss and dramatic deterioration of mechanical properties. Thus, enhancing the thermal stability of SiOC glasses is still an ongoing task. Riedel et al.[8] and Kroke et al.[9] reported that boron doped silicon carbonitride (SiCNB) glasses got the improved thermal stability properties, which greatly inspired the SiOC glasses researchers. The incorporation of boron into silicon oxycarbid network was found to inhibit the formation of cristobalite[10,11] and lead to the growth of $[B(OSi)_3]$ units, reduction of $[SiO_4]$ units and enhancement of SiC crystallization.[12,13] The most important effect is that the decomposition temperature of boron addition silicon oxycarbid glasses increases at least up to 1400 °C.[12,14] Therefore, the SiBOC ceramic products, including fibers, derived from boron addition silicon oxycarbid are promising candidates for high temperature applications.[15]

It is well known that the chain-like or linear-type polymers are required for the fiber-forming. Although the borosiloxanes as precursors for SiBOC ceramics are successfully synthesized from modified silicon alkoxide[16,17] and cyclic siloxane[18], the spinnability of these borosiloxane precursors is poor because of the lack of chain-structure in the polymers. In order to overcome this shortcoming, Peña-Alonso et al.[19] prepared hydrid borosiloxane gels using $B(OH)_3$ and mixture of MTES and DMDES. The formation of linear oligomers was promoted by

* Corresponding author at: School of Materials Science and Engineering, Harbin Institute of Technology, Harbin 150001, PR China.
Tel.: +86 451 8641 8860; fax: +86 451 88641 3922.
E-mail addresses: g.w.wen.hit@gmail.com, g.wen@hit.edu.cn (G. Wen).

0955-2219/$ – see front matter © 2010 Elsevier Ltd. All rights reserved.
doi:10.1016/j.jeurceramsoc.2010.11.020

Table 1
Composition, aspects of dried gels and spinnability of the precursor sols.

Samples	PMES (ml)	$B(OH)_3$ (g)	Ethanol (ml)	Aspects	Spinnability
S0.1	50	3.4	1.8	Transparent	Perfect, ~3 m
S0.2	50	6.8	4.2	Transparent	Perfect, ~4 m
S0.4	50	13.6	6.8	Opaque	Good, ~80 cm
S0.6	50	20.4	9.5	Opaque, deposit	Able, ~30 cm

the difunctional silicon units $–(CH_3)_2SiO–$, which was favorable to fabricate long SiBOC fibers by hand-drawing. However, it is hard to result in ideal compositional and structural homogeneities in the final ceramics by physical mixing of different polymers.[20] Thus, it is highly desirable to develop and explore single-source precursors with excellent spinnablity for SiBOC fiber-forming.

In the present work, SiBOC gel fibers have been successfully fabricated from single-source polyborosiloxanes which are synthesized from polymethylethoxysiloxane (PMES) and $B(OH)_3$ by a sol–gel process, and SiBOC ceramic fibers have been obtained by subsequent thermolysis in argon atmosphere. The morphological change, chemical mechanism and structural evolution of the fibers starting from gels to ceramics during heat treatment are investigated. In addition, the crystallization behavior between 1000 and 1500 °C is studied by X-ray diffraction and Raman spectroscopy to obtain the structural information on the various SiBOC ceramic fibers.

2. Experimental procedures

2.1. Synthesis of precursor

The linear polymethylhydrogensiloxane (PMHS), $(CH_3)_3Si(CH_3(H)SiO)_m$, was purchased from Shin-etsu Chemical Co., Ltd. Absolute ethyl alcohol, ethylenediamine and boric acid were supplied by Tianjin Kermael Chemical Reagents Evelopment Centre, China. All the reagents were used as received without further purification.

The synthesis of hybrid borosilicate precursors was preformed in two steps: (1) preparation of PMES and (2) synthesis of polyborosiloxane gel by sol–gel method.

0.3 ml of ethylenediamine was added into the mixture of 100 ml of PMHS and 120 ml of ethanol under magnetic stirring. The dehydrogenation reaction between PMHS and ethanol under catalysis of ethylenediamine was carried out at ambient temperature for 20 days, which was accompanied by the evolution of hydrogen. After elimination of residual ethanol under reduced pressure, 175 ml of PMES was isolated as colorless liquid.

The polyborosiloxane gels were synthesized according to the following procedure: PMES and $B(OH)_3$ were mixed and heated to 78 °C. Then ethanol was gradually added into the mixture until the $B(OH)_3$ was completely dissolved under stirring. The transparent reaction mixture was kept under reflux at 78 °C until the precursor sol became viscous. Then, the sol was poured into plastic containers and was left open at ambient temperature for gelation. Four sets of sol solutions with B/Si molar ratio of 0.1, 0.2, 0.4 and 0.6 were prepared. Table 1 lists the composition of the sol solutions and the aspect of the gels.

2.2. Fiber preparation

Spinnability of the sols was estimated by regularly dipping a glass stick 3 mm in diameter and pulling it up quickly during the aging of the sol solutions. It was found that gel fiber was obtained successfully in all four partially aged solutions before complete gelation. The obtained fibers were gelled in the ambient environment for 4 days and dried at 70 °C for 4 days before thermolysis. Four SiBOC gel fiber systems with a nominal B/Si atomic ratio of 0.1, 0.2, 0.4, and 0.6 were prepared, which were labeled as S0.1, S0.2, S0.4 and S0.6, respectively. The spinnability of polyborosiloxane precursor sols with different boron contents is displayed in Table 1. Heat treatments of green fibers were performed in argon atmosphere at various temperatures between 300 and 1500 °C with a heating rate of 2 °C/min. Heating was then automatically turned off after holding at the final temperature for 1 h and the samples were cooled to room temperature.

2.3. Characterization techniques

FT-IR spctra were recorded on a Bruker Vector 22 spectrophotometer, using KBr pellets for solid samples and liquid film on NaCl wafer for liquid samples, from 400 to 4000 at resolution of 4 cm^{-1}. Molecular weight distributions and molecular weights were estimated by gel permeation chromatography (GPC) using Waters 515 HPLC pump (THF, 1.0 ml/min, 35 °C) equipped with Styragel HT3 and HT4 columns in series with Waters 2414 RI Detector. The morphology of the green gel fibers and ceramic fibers was observed by scanning electron microscopy (SEM, MX2600EF). X-ray diffraction was conducted by Rigaku *D*/max-γB diffractometer with Cu K_α radiation ($\lambda = 0.154178$ nm) at a scan speed of 4° min^{-1}. Thermal gravimetric analysis (TGA, on Netzsch STA) was carried out in argon atmosphere from 30 to 1500 °C at a heating rate of 5 °C/min in alumina crucible. The gas decomposition during thermolysis was identified in a continuous process using a mass spectrometry (Omnistar^{TM}) between 30 and 1000 °C. For X-ray photoelectron spectroscopy (XPS), powder samples were analyzed by a physical Electronics PHI 5700 ESCA system with an exiting source of Mg ($K_\alpha = 30$ eV). The structure evolution of free carbon was investigated by Raman spectroscopy (Jobin-Yvon HR800) using an Ar-ion laser with an energy of 2.71 eV ($\lambda = 457.9$ nm).

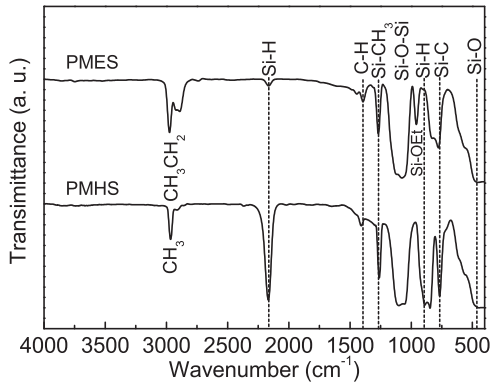

Fig. 1. FT-IR spectra of PMHS and as-synthesized PMES.

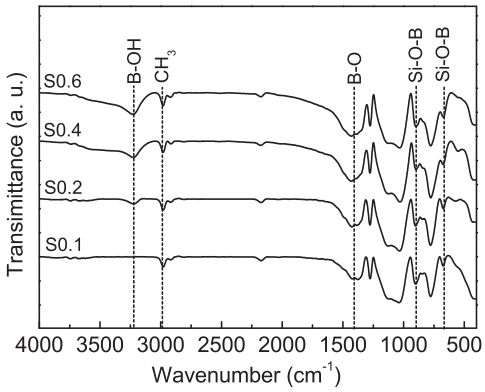

Fig. 2. FT-IR spectra of dried fibrous gel S0.1–0.6.

3. Results and discussion

3.1. Characterization of polymethylethoxysiloxane

FT-IR spectra (Fig. 1) show that the PMES is characterized by different features with respect to PMHS. Most of the Si–H groups (2170 and 877 cm^{-1}) are consumed in PMES, which is further confirmed by the evolution of hydrogen during the reaction process. A new band at 956 cm^{-1} due to ≡Si–OEt (Et=CH_3CH_2–) stretching vibration[21] is observed in PMES. Three peaks are detected in the range of 2975–2890 cm^{-1}: CH_3 asymmetric stretching at 2975 cm^{-1}, the combination between the CH_3 symmetric and the CH_2 asymmetric stretching at 2923 cm^{-1}, CH_2 symmetric stretching at 2890 cm^{-1}, which confirm the presence of CH_3CH_2– groups in PMES.[22] The strong Si–O absorption at 1080 cm^{-1} with a shoulder at 1120 cm^{-1} is characteristic of linear Si–O–Si chains.[23,24] Molecular weights and molecular weight distributions of PMHS and PMES were examined by GPC. The molecular weights of PMES (M_w = 3426, M_n = 2815) are lower than that of PMHS (M_w = 8361, M_n = 5196). According to the number average molecular weight (M_n), the polymerization degrees of PMHS and PMES are about 80 and 30, respectively. Above results indicated that PMES was obtained based on dehydrogenation reaction, as shown in Scheme 1. Si–H groups of PMHS react with O–H groups of ethanol to give off hydrogen under catalysis of ethylenediamine and CH_3CH_2O– functional groups homogenously incorporate into the linear Si–O–Si backbone of PMES. It is noteworthy that molecular weight distribution of the PMES is narrow (M_w/M_n = 1.2), which is favorable for fabricating homogenous gels, as revealed in the later section.

3.2. Characterization of SiBOC gel fibers

Polyborosiloxane gel fibers with various B/Si atomic ratios are systematically investigated. The FT-IR spectra of four dried gel fibers S0.1–0.6 are illustrated in Fig. 2. The peaks located at 895 and 675 cm^{-1} attributed to the borosiloxane bridges (≡Si–O–B)[16] are distinctly identified in all final gels. The presence of ≡Si–O–B bridges indicates that the polyborosiloxane gels were successfully synthesized from PMES and $B(OH)_3$, in which trigonal BO_3 units were incorporated into the siloxane network via Si–O–B bridges.[17] Additionally, the B–O groups at 1500–1300 cm^{-1} and the B–OH groups at 3224 cm^{-1} are present in gels.[16,25] Reactions (1)–(3) might be the possible way leading to the formation of ≡Si–O–B bridges in the network.[17,26] Reaction (1) occurs first followed by reaction (2), as revealed by the research of Irwin,[26] while reaction (3) may play a minor role in the sol system because the presence of excess ethanol would drive equilibrium to left. Furthermore, the FT-IR spectra show CH_3– groups is instead of CH_3CH_2– groups in polyborosiloxane gels compared with PMES. The residual CH_3CH_2O–Si bonds are reduce by hydrolysis and as-obtained Si–OH moieties condense to form siloxane network during the sol–gel process,[18] as shown in reaction (4) and (5). Therefore, the CH_3– groups originating from PMHS are merely detected in the dried gels. The bands located at 1135 and 1035 cm^{-1} are attributed to SiOSi-cage and SiOSi-network absorptions,[27] respectively, which further suggest that three-dimensional network structure has successfully built up in the SiBOC gels. As also displayed in Fig. 2, the relative intensity of ≡Si–O–B bridges, B–O and B–OH groups shows an increasing tendency when the boron content is increased, while the relative intensity of ≡Si–O–B

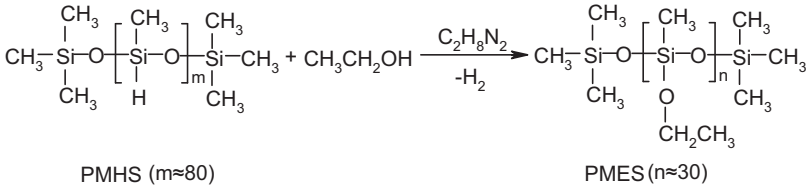

Scheme 1. Synthesis of PMES from PMHS.

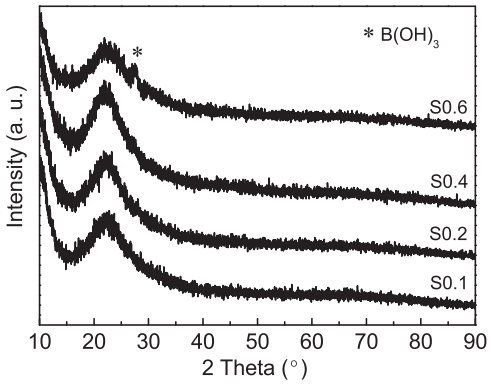

Fig. 3. XRD pattern of dried fibrous gel S0.1–0.6.

bridges of S0.6 gel is similar to that of S0.4 gel.

$$=B–OH + EtO–Si\equiv \rightarrow =B–O–Et\equiv + OH–Si\equiv \quad (1)$$

$$=B–OH + HO–Si\equiv \rightarrow =B–O–Si\equiv + H_2O \quad (2)$$

$$=B–OH + EtO–Si\equiv \rightarrow =B–O–Si\equiv + EtOH \quad (3)$$

$$Si–OEt + H_2O \rightarrow Si–OH + EtOH \quad (4)$$

$$Si–OH + OH–Si \rightarrow Si–O–Si + H_2O \quad (5)$$

Fig. 3 shows XRD patterns collected from polyborosiloxane gels with different boron contents. The spectra of S0.1–0.4 gels display a completely amorphous structure with only the presence of SiO_2 halo centered at $2\theta \approx 22^\circ$. Whereas another weak diffraction peak at $2\theta = 28^\circ$ corresponding to crystalline $B(OH)_3$ (JCPDS 23-1034) is present in S0.6 gel. Indeed, white precipitation of $B(OH)_3$ can be clearly observed in S0.6 system during the sol–gel process. The FT-IR and XRD results indicate that the amount of ≡Si–O–B bridges would be promoted up to a certain level with the increase of boron content. When the B/Si atomic ratio increases from 0.4 to 0.6, the further boron addition would form a secondary $B(OH)_3$ rich phase, owing to the steric hindrance within the polymer.

Fig. 4 shows the SEM images of the hand drawn SiBOC gel fibers, reflecting the diverse spinnability of polyborosiloxane sols with different B/Si atomic ratios. The fibers with length up to several meters were easily obtained by hand drawing from partial aged S0.1 and S0.2 sols with appropriate viscosity, and the sol solutions kept homogenous and transparent during gelation (Table 1). Fig. 4a and b show the morphologies of the as-obtained S0.1 and S0.2 gel fibers. Uniform gel fibers possess smooth and dense appearances without pores and defects. The cross-sections of these dried gel fibers are circular in shape with diameters ranging from 10 to 30 μm. The superior spinnability of these two sols is attributed to the high degree of polymeric cluster structures originating from Si–O linear chains in PMES. However, the spinnability of sols is remarkably dependent on the boron content. For S0.4 sol solution, the spinnability is weakened due to the development of higher networked structure. In addition, the slight agglomerate of $B(OH)_3$ is observed in the S0.4 sol solution with appropriate viscosity, which is a disadvantage to prepare uniform fibers (Fig. 4c). Still, gel fibers of about 80 cm in length were obtained. In the case of S0.6 sol, the deposition of un-reacted $B(OH)_3$ is heavily developed in the sol solution, which not only makes it difficult to control the composition of

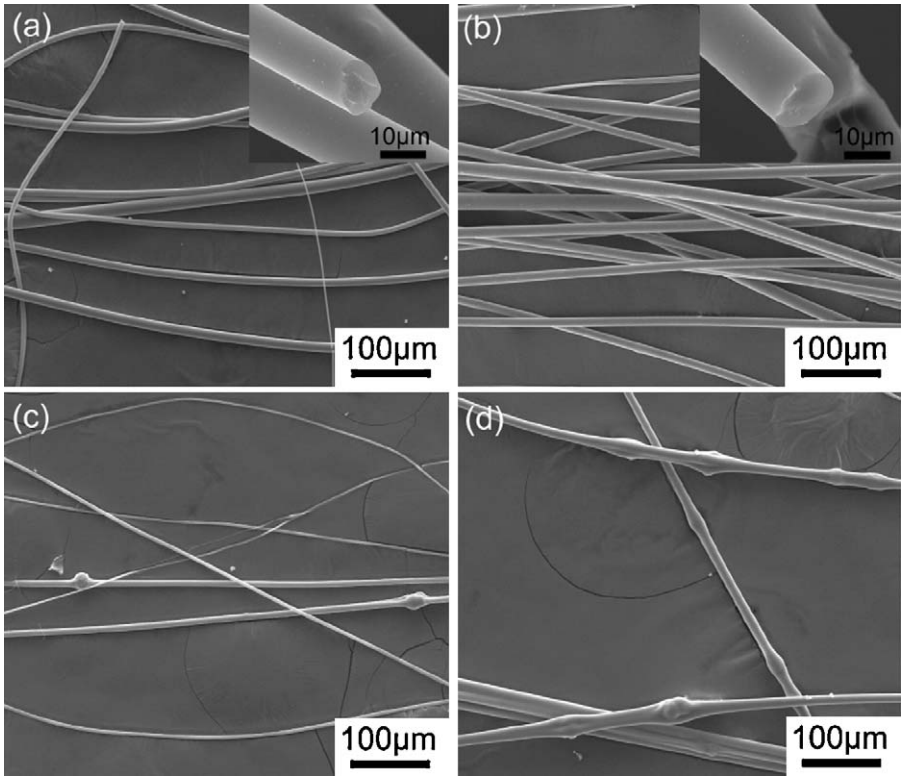

Fig. 4. SEM micrographs of the surface morphology of gel fibers. (a) S0.1 (insert: cross-section view), (b) S0.2 (insert: cross-section view), (c) S0.4 and (d) S0.6.

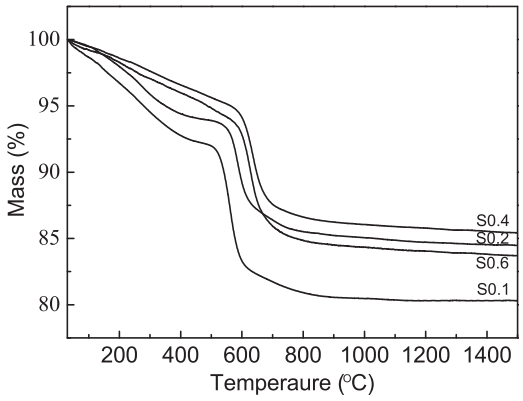

Fig. 5. TG profiles of S0.1–0.6 gel fibers up to 1500 °C.

final gel but also deteriorates the spinnability. Lots of knobs are clearly observed in the S0.6 gel fibers (Fig. 4d). Therefore, it is reasonable to conclude that S0.1 and S0.2 are the promising systems for the preparation of continuous SiBOC fibers.

3.3. Polymer-to-ceramic conversation

Fig. 5 depicts the thermogravimetric (TGA) curves of S0.1–0.6 gel fibers up to 1500 °C. Thermal decomposition of the gel fibers is featured by continuous weight loss in two stages. The first weight loss stage is observed from room temperature to about 520 °C (S0.1 and S0.2) or 600 °C (S0.4 and S0.6) with the weight loss of 8.2, 6.6, 5.4 and 6.3 wt.% for S0.1, S0.2, S0.4 and S0.6, respectively. The second weight loss stage ends around 800 °C in one single reaction step leading to a weight loss of 10.6, 8.3, 7.5 and 8.0 wt.%, respectively. Consequently, the ceramic yields at 1000 °C are 80.5, 85.1, 86.0 and 84.3 wt.% for sample S0.1, S0.2, S0.4 and S0.6, respectively. The weight loss of the S0.1–0.4 gels decreases with increasing boron content due to the increase of the degree of the gels cross-linking which leads to a more condensed network, while the weight loss of S0.6 is higher than that of S0.4 probably due to the presence of the secondary $B(OH)_3$ rich phase. The evolution of H_2O from the B–OH moieties at low temperature (below 300 °C) and the influence of the resultant B_2O_3 on the redistribution and mineralization reactions between 300 and 800 °C might be responsible for the higher weight loss of S0.6 gel than S0.4 gel. These results imply that the boron content and the cross-linking degree prominently affect the thermolysis behavior of the precursor gels. In the temperature interval ranging from 1000 to 1500 °C, the samples show slight mass losses (<0.5 wt.%), which most probably result from the evaporation of gaseous silicon monoxide. The very limited mass losses suggest that carbothermal reduction is not active and redistribution reactions play the main role to cause structure evolution. It is noteworthy that the SiBOC gels exhibit ideal high ceramic yield, which is beneficial to the production of dense ceramic fibers.

The thermolysis behavior of polyborosiloxane gel fibers was further investigated by TG/MS operated between room temperature and 1000 °C. The S0.4 gel fiber was used as a representative sample. As shown in Fig. 6, H_2O ($m/e = 18$) and ethanol ($m/e = 31$) release in the temperature range of

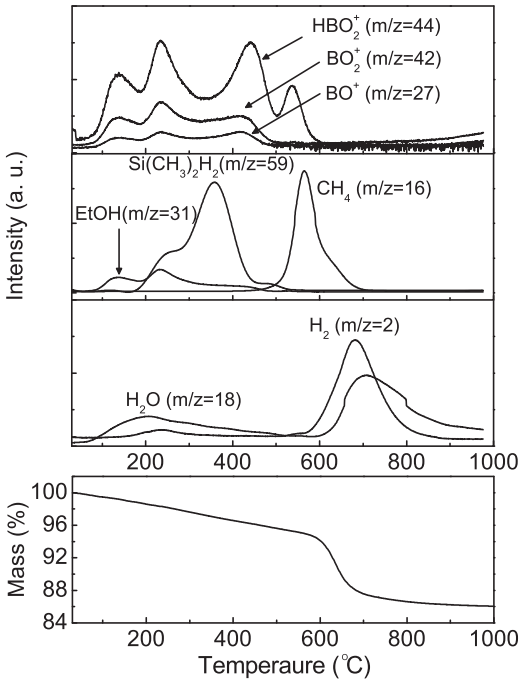

Fig. 6. TG/MS profiles of S0.4 gel fiber pyrolyzed at 5 °C/min, under Ar up to 1000 °C.

80–300 °C due to condensation of the residual Si–OH, Si–OEt and B–OH bonds. In addition, fragment units of HBO_2^+ ($m/e = 44$), BO_2^+ ($m/e = 42$) and BO^+ ($m/e = 27$) are observed in this temperature range resulting from evaporation of volatile boron compounds.[28,29] Between 200 and 300 °C, a small amount of H_2 ($m/e = 2$) and $Si(CH_3)_2H_2$ ($m/e = 59$) is detected, which mainly results from the dehydrocoupling reaction of residual Si–H groups and redistribution of Si–O/Si–H bonds,[30,31] respectively. At higher temperature ranging from approximate 300 to 600 °C, a second thermal decomposition occurs with evaporation of $Si(CH_3)_2H_2$ and fragment units of HBO_2^+, BO_2^+ as well as BO^+. The low molecular weight Si-containing volatile species $Si(CH_3)_2H_2$ is attributed to the Si–O/Si–C redistribution reactions,[30] and the boron-containing fragment units might be ascribed to partial Si–O–B bridges breaking.[21] CH_4 ($m/z = 16$) shows a broad evolution band in the temperature range of 500–700 °C, and H_2 is detected from 600 to 1000 °C. The evolution of CH_4 and H_2 is accounted for the mineralization reaction,[30,32] involving the following reaction: hemolytic cleavage of Si–C and C–H bonds, and abstraction of H_2 by the radicals from the C–H groups. The detection of H_2O from 600 to 1000 °C might be due to the oxidation of hydrogen[33] or homolytic cleavage of Si–O bonds.[32] According to these results, we can assume that the conversation of polyborosiloxane into an inorganic glass is achieved at 1000 °C.

The B/Si atomic ratios calculated from XPS spectra for S0.1–0.6 gels fibers and corresponding ceramic fibers are listed in Table 2. B/Si atomic ratio of starting gels is slightly lower than the theoretical value, which is ascribed to the evaporation of boron containing species during the sol–gel process and drying.[34] At 1000 °C, the decrease of B/Si atomic ratio is detected in ceramics compared with gels, which further confirms

Table 2
The B/Si atomic ratio for S0.1–0.6 gels fibers and corresponding ceramic fibers, as obtained from XPS spectra.

Samples	B/Si atomic ratio at gel	B/Si atomic ratio at 1000 °C	B/Si atomic ratio at 1500 °C
S0.1	0.09	0.05	0.07
S0.2	0.21	0.13	0.14
S0.4	0.38	0.28	0.30
S0.6	0.54	0.35	0.36

the evaporation of boron compounds during the thermolysis as revealed by mass spectroscopy. Up to 1500 °C, the B/Si atomic ratio presents a faint increasing tendency, suggesting that a small amount of silicon compound such as gas silicon monoxide evaporates. However, the weight loss is very limited and the formation of volatile species (SiO, CO) is not active.

The structure evolution from precursor gel to ceramic with respect to thermolysis temperatures was monitored by the means of FT-IR (Fig. 7). The S0.4 gel fiber and the corresponding ceramic fiber were taken as representative samples. After heat treatment at 300 °C, the peaks originating from B–OH groups at 3200 cm^{-1} and Si–H groups at 2100 cm^{-1} disappear in both samples, while the relative intensity of ≡Si–O–B bridges is comparable to that in gels. Heat treatment at 600 °C is sufficient to promote redistribution reaction between Si–O and Si–C groups, reflected by the decreasing in intensity of Si–CH_3 bands. Si–CH_3 band at 2970 cm^{-1} and C–H band at 2910 cm^{-1} are completely consumed up to 800 °C, implying that the mineralization reaction occurs accompanying with the release of H_2 and CH_4, as detected by mass spectroscopy. It is noted that the peaks due to the ≡Si–O–B bridges at 895 and 675 cm^{-1} remarkably diminish at thermolysis temperatures beyond 300 °C. After heat treatment at 1000 °C, the spectrum is characterized by the following typical bands: Si–O at 1080 and 460 cm^{-1}, Si–C at 800 cm^{-1}, B–O at 1400 cm^{-1} and Si–O–B at 895 and 675 cm^{-1}. This confirms the complete consumption of the initial precursor gel and the formation of inorganic network. In the ceramics obtained at 1300 and 1500 °C, progressive increasing of the ≡Si–O–B bridges at

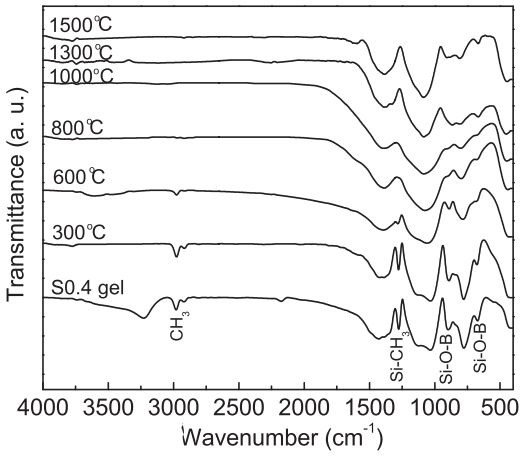

Fig. 7. FT-IR spectra of S0.4 fibers at r.t. 300, 600, 800, 1000, 1300 and 1500 °C.

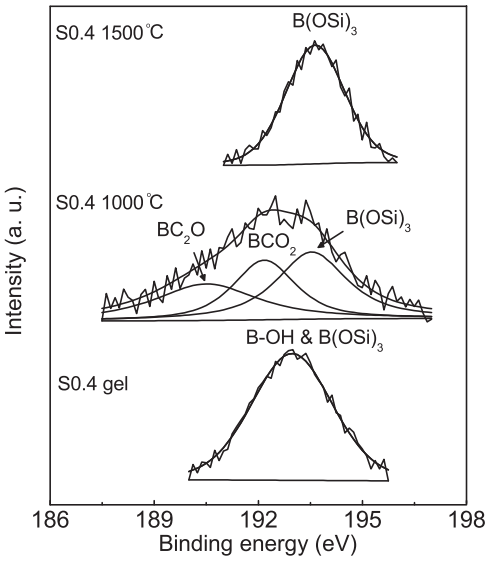

Fig. 8. XPS spectra of B 1 s taken on the S0.4 fibers at r.t., 1000 and 1500 °C.

895 and 675 cm^{-1} is verified, indicating that the structure modification of the residue obtained at 1000 °C takes place through redistribution reaction at higher thermolysis temperatures.

To correlate the results obtained from FT-IR spectroscopy of these samples, we further analyzed the structure evolution by XPS analysis. Fig. 8 shows the high-resolution XPS spectra of B 1s taken on the S0.4 sample. The B 1s spectrum of S0.4 gel fiber consists of one signal at 193.0 (±0.1) eV. This value is close to the binding energy of boric acid (192.8 eV), thus we assign this signal to the combination of ≡B–O–Si and B–OH units considering the presence of those groups in the gel as verified by the FT-IR analysis (Fig. 2). Another two distinct signals appear in S0.4 ceramic fiber at 1000 °C, i.e. BC_2O at 190.1 (±0.2) eV and BCO_2 at 192.0 (±0.2) eV.[35] In addition, the binding energy of ≡B–O–Si units shifts up to 193.5 (±0.1) eV, which shows the presence of borosilicate structure in the network.[36] The presence of BC_xO_{3-x} ($0 \le x \le 2$) units in XPS spectrum and the diminution of Si–O–B bridges in FT-IR spectrum at 1000 °C indicate that Si–O–B bridges are partially replaced by B–C bonds and the BC_xO_{3-x} units are present in the network, which is in agreement with that reported by Gervais et al.[37] After annealed at 1500 °C, the BC_xO_{3-x} units are completely consumed and the signal at 193.5 (±0.1) eV is associated with trigonal borosilicate ($B(OSi)_3$) units. The presence of boron in the glass network is favorable for the redistribution reaction involving boron oxycarbide (BC_xO_{3-x}) and silicon oxycarbid (SiC_xO_{4-x}) units to form SiC nuclei and borosilicate glassy clusters above 1200 °C.[12] This phase evolution is more pronounced with higher thermolysis temperature and boron content for SiBOC glass. Fig. 9 presents the high-resolution XPS spectra of Si 2p taken on the S0.2 and S0.4 ceramic fibers pyrolyzed at 1500 °C. Both Si 2p XPS signals have been Gaussian simulated with the contribution of SiO_4 units at 103.6 (±0.1) eV and SiC_4 units at 100.8 (±0.1) eV. Thus, the SiBOC ceramics annealed at 1500 °C might be described as a mixture mainly composed of trigonal $B(OSi)_3$, SiO_4 and SiC_4 units.

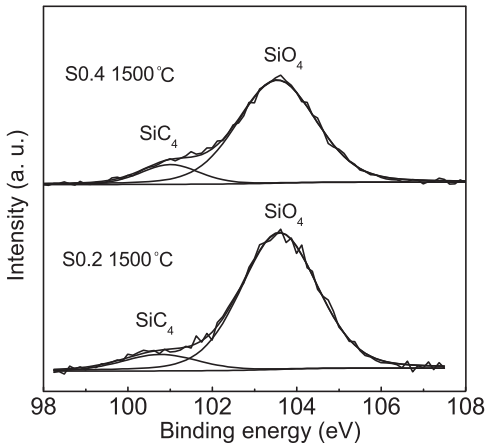

Fig. 9. XPS spectra of Si 2p taken on the S0.2 and S0.4 ceramic fibers pyrolyzed at 1500 °C.

3.4. Morphology change of SiBOC ceramic fibers

Green fibers (S0.1, S0.2 and S0.4) were pyrolyzed to produce black ceramic SiBOC fibers at 1000, 1300 and 1500 °C. The ceramic fibers obtained at 1000 °C (Fig. 10a, d and g) and 1300 °C (Fig. 10b, e and h) have smooth and defect-free surface. The cross-sections of these fibers show the circular characteristic with a diameter of about 10 μm. The dense texture with glass-like cross section indicates an amorphous state of the ceramic fibers at 1000 °C. After annealed at 1300 °C, the glass-like texture of S0.1, S0.2 and S0.4 ceramic fibers is still retained. The appearance of a rough surface in the S0.1 ceramic fibers annealed at 1500 °C (Fig. 10c) might be related with the occurrence of carbothermal reduction accompanied with loss of gaseous reaction products such as SiO and CO through the surface, which is agreement with B/Si atom ratio evolution and TG analysis. In comparison, there is no evident decomposition trend in the S0.2 and S0.4 ceramic fibers after heat treatment at 1500 °C (Fig. 10f and i). Thus, the boron introduction can effectively inhibit carbothermal reduction. However, the cross-section boundary of S0.4 ceramic fiber is illegible, indicating that the S0.4 ceramic fiber might melt at about 1500 °C. It is known that the presence of borosilicate richer in boron will lead to the lower viscosity of SiBOC glass.[12,13] As a result, the S0.4 ceramic fiber with B/Si atom ratio of 0.30 might melt at 1500 °C, while the S0.2 ceramic fibers with B/Si atom ratio of 0.14 are thermal stable at 1500 °C. Therefore, appropriated boron content in SiBOC ceramic fibers is necessary for improving the high-temperature stability.

3.5. Crystallization tendency of SiBOC fibers

Fig. 11 presents the XRD patterns recorded on the samples thermolyzed at 1300 and 1500 °C. The S0.1–0.6 ceramic fibers at 1000 °C are completely amorphous (not shown here). At 1300 °C, in addition to silica halo centered at about $2\theta = 22°$, diffraction peaks of β-SiC (JCPDS 29-1129) at $2\theta = 35°$ (1 1 1), 60° (2 2 0) and 72° (3 1 1) start to appear for the four sam-

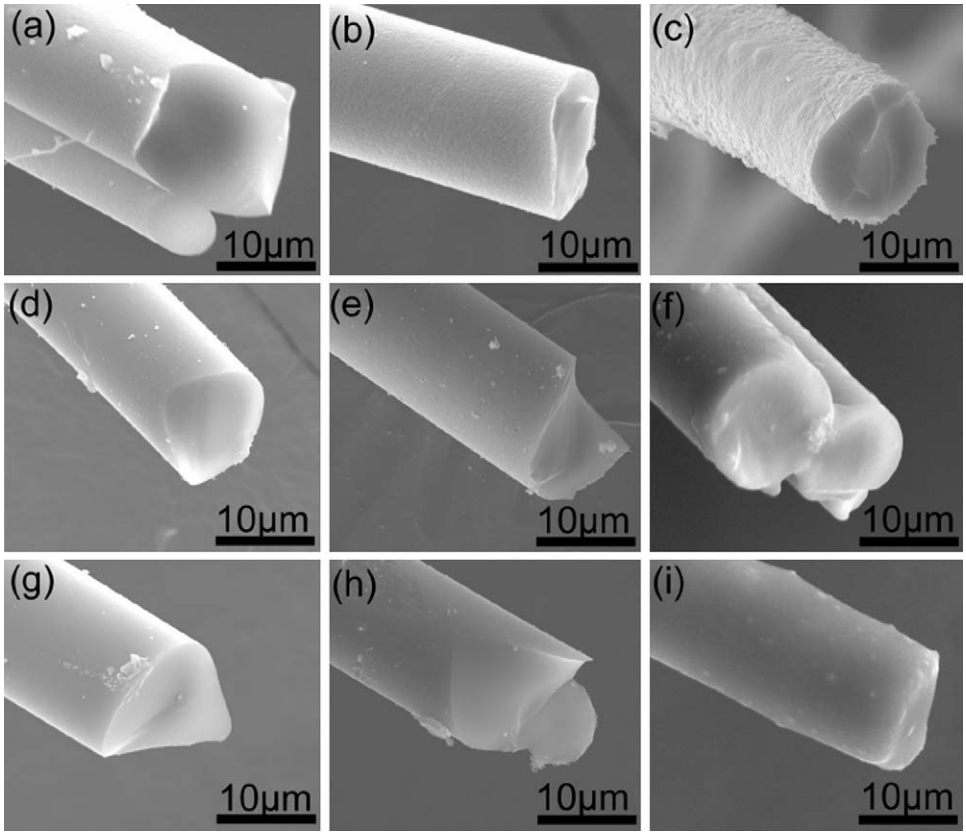

Fig. 10. SEM micrographs of the cross-sections of S0.1 ceramic fiber annealed at (a) 1000, (c) 1300, (e) 1500 °C; S0.2 ceramic fibers annealed at (b) 1000, (d) 1300, (f) 1500 °C and S0.4 ceramic fibers annealed at (g) 1000, (h) 1300, (i) 1500 °C.

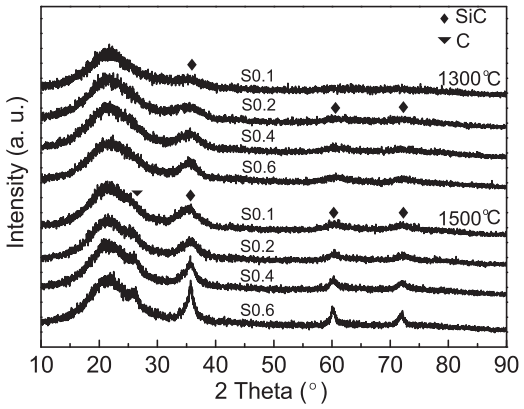

Fig. 11. XRD patterns of S0.1–0.6 ceramic fibers pyrolyzed at 1300 and 1500 °C.

ples. At 1500 °C, all these peaks become sharper, indicating that the increase of themolysis temperature promotes the crystallization of β-SiC. The mean crystal size of β-SiC, calculated from the width of the (1 1 1) diffraction peaks at mid height according to Scherre equation, is reported in Table 3. The data shows β-SiC nanocrystals grow with increase of pyrolysis temperature and the content of boron in SiBOC samples. Furthermore, shoulder peaks at $2\theta = 26.6°$ due to (0 0 2) reflection of graphite carbon (JCPDS 26-1080) are present in all the four samples at 1500 °C. It is also found that the boron promotes the graphitization of nanocrystalline graphite. These effects are probably due to the reduction of viscosity because the presence of borosilicate units in the network increases the diffusion rate for crystallization.[12,13] Furthermore, there is no crystalline silica detected in the samples thermolyzed at 1300 and 1500 °C. Thus, the transformation from α- to β-cristobalite structure, accompanying a large volume change and sometimes causing microcrack formation during cooling, can be inhibited.

Raman spectroscopy was employed to further examine the structural evolution of free carbon phase of S0.2 and S0.4 ceramic fibers thermolyzed at 1000, 1300 and 1500 °C. As shown in Fig. 12, the Raman spectra of all samples show several characteristic features, the so-called G and D bands appeared in the first-order region (1100–1800 cm^{-1}) around 1550–1570 cm^{-1} and 1340–1360 cm^{-1}, respectively, as well as the G′ bands located in the second-region (2200–3400 cm^{-1}) around 2700 cm^{-1} for visible excitation.

For the nanographite samples, the integrated intensity of D and G mode ratio, I_D/I_G, is inversely proportion to the in-plane carbon crystallite size L_a. A general equation for the relation of the crystallite size L_a and the excitation laser energy was given as follows:[38]

$$L_a\,(\mathrm{nm}) = \frac{560}{E_l^4}\left(\frac{I_D}{I_G}\right)^{-1}$$

where E_l is the excitation laser energy used in the Raman experiment in the eV unit. The value of excitation laser energy here is 2.71 eV. In order to determine the evolution of free carbon phase during the heat treatment, Lorentzian curve fitting of Raman bands after linear baseline correction was performed to extract the useful spectra parameters of studied samples which are reported in Table 4.

Table 3
Crystallite size of β-SiC crystals pyrolyzed at 1300 and 1500 °C.

Samples	$D_{SiC(1\,1\,1)}$ (nm)	
	1300 °C, 1 h	1500 °C, 1 h
S0.1	1.1 ± 0.2	2.1 ± 0.2
S0.2	1.8 ± 0.2	3.2 ± 0.2
S0.4	2.0 ± 0.2	4.5 ± 0.2
S0.6	2.5 ± 0.2	6.4 ± 0.2

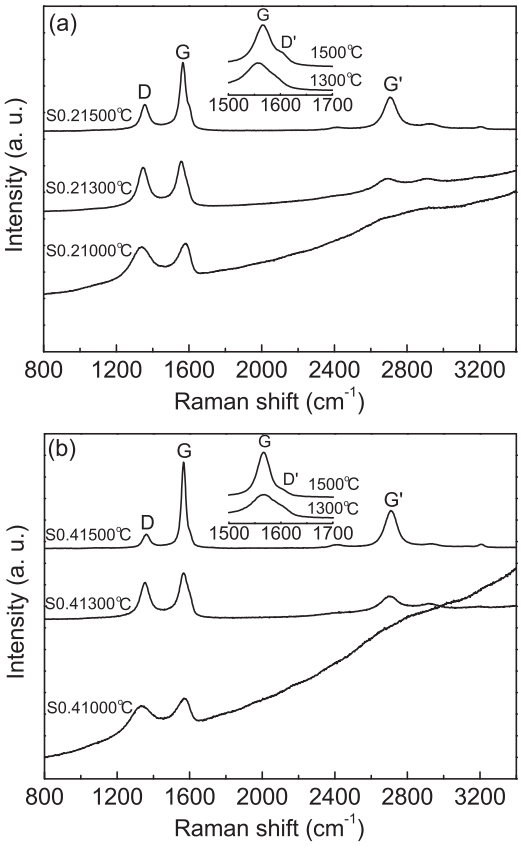

Fig. 12. Raman spectra of (a) S0.2 ceramic fibers and (b) S0.4 ceramic fibers pyrolyzed at 1000, 1300 and 1500 °C (inset: an enlargement view of range between 1500 and 1700 cm^{-1}).

In general, the heat treatment promotes a shift to higher vibration frequencies and a reduction of full width half maxima of the G, D and G′ band. The ratio of D and G band integrated intensity (I_D/I_G) decreases with increasing temperature. Consequently, the heat treatment gives rise to the increase of the in-plane carbon crystallite size L_a of free carbon. At 1500 °C, the fluorescence background disappears and very distinct and narrow D and G bands are observed in the samples. The frequency of G bands of S0.2 and S0.4 are 1567 and 1568 cm^{-1}, respectively, close to the G mode of graphite at 1581 cm^{-1}.[39] In addition, new shoulder peaks at 1605 cm^{-1} are observed in the samples at 1500 °C (inset in Fig. 10), which might be corresponding to disorder-induced D′ band frequently appearing in the nanocrystalline graphite.[40] This band indicates that some C atoms of graphene plane are substituted by B atom with the

Table 4
The band characteristics (peak position, full width at half maxima, I_D/I_G and carbon crystallite size) of Raman spectra.

Samples	Temperature (°C)	D (cm^{-1})	H_D (cm^{-1})	G (cm^{-1})	H_G (cm^{-1})	G′ (cm^{-1})	$H_{G'}$ (cm^{-1})	I_D/I_G	L_a (nm)
S0.2	1000	1338	120	1550	65	–	–	2.49	4.2
	1300	1348	87	1556	62	2690	134	1.07	9.7
	1500	1356	70	1567	45	2707	83	0.51	20.4
S0.4	1000	1330	183	1563	68	–	–	2.01	5.2
	1300	1352	69	1565	63	2700	122	0.83	12.5
	1500	1360	50	1568	30	2709	75	0.26	39.9

formation of BC_3 units.[13] The second-order G′ bands, sensitive to the stacking order of the graphene sheets along the *c*-axis,[40] become well defined up to 1500 °C and can be fit using only one single Lorentzian peak centered at 2707 and 2709 cm^{-1}, respectively, for S0.2 and S0.4 samples. This is the typical profile of the G′ band of turbostratic graphite samples which have no stacking order and can be considered as 2D nanographite systems.[41] In addition, the integrated intensity of G′ band increases in samples during annealing, and this is a reflection of increase of in-plane crystallite size L_a.[37] These evolutions suggest that, for SiBOC ceramics, significant ordering process of free carbon phase takes place during annealing and the turbostratic graphite is formed at 1500 °C. It is noted that the boron-content of SiBOC ceramic has a remarkable effect on the crystalline of free carbon (sp^2 C phase). At the same temperature, the in-plane carbon crystallite size L_a of the S0.4 sample is larger than that of the S0.2 sample. In addition, other spectra parameters also indicate that the ordering process of the free carbon phase in S0.4 samples is more efficient than that in S0.2, as confirmed by the above XRD analysis.

4. Conclusion

In this study, SiBOC ceramic fibers have been successfully fabricated using newly developed polyborosiloxane precursors, which are synthesized via a facile sol–gel route using polymethylethoxysiloxane (PMES) and $B(OH)_3$ as starting materials. The PMES, a linear-type polymer obtained by the alcoholysis of polymethylhydrogensiloxane, is an effective starting material to the synthesis of SiBOC precursor with remarkable spinnability. Boron content not only influences the spinnability of polyborosiloxane sols but also affects the thermolysis and crystallization behavior of fibers. Long gel fibers are easily obtained from polyborosiloxane sols with B/Si atom ratio of 0.1 and 0.2 by hand drawing. Dense and crack-free SiBOC ceramic fibers with a diameter of about 10 μm are prepared by pyrolysis at 1000 °C with high ceramic yield ranging from 80.5 to 86.0%. SiBOC ceramic fibers with B/Si of 0.14 are thermal stable up to 1500 °C. The structural evolution of SiBOC fibers monitored by FT-IR and XPS spectroscopy reveals that the continuous structure rearrangement within ceramic fibers takes place with increasing pyrolysis temperature. The SiBOC ceramic network is composed of mixed SiC_xO_{4-x}, BC_xO_{3-x} and $B(OSi)_3$ units at 1000 °C, which evolves to $B(OSi)_3$, SiC_4, SiO_4 units and turbostratic graphite at higher temperature up to 1500 °C. The crystal growth tendency of both β-SiC and free carbon is strengthened with the increase of boron content and pyrolysis temperature. Boron leads to ordering of sp^2 C phase and formation of turbostratic graphite at 1500 °C. The SiBOC ceramic fiber developed here is a promising candidate for high temperature applications.

Acknowledgements

This work was supported by National High-tech R&D Program of China (863 Program) (No. 2007AA03Z340), National Science Foundation of China (No. 50672018) Fundamental Research Funds for the Central Universities (HIT. ICRST. 2010009) and Program of Excellent Team in Harbin Institute of Technology.

References

1. Bunsell AR, Berger MH. Fine diameter ceramic fibers. *J Eur Ceram Soc* 2000;**20**:2249–60.
2. Sorarù GD, Modena S. Chemical durability of silicon oxycarbide glasses. *J Am Ceram Soc* 2002;**85**:1529–36.
3. Moysan C, Riedel R, Harshe R, Rouxel T, Augereau F. Mechanical characterization of a polysiloxane-derived SiOC glass. *J Eur Ceram Soc* 2007;**27**:397–403.
4. Bréquel H, Parmentier J, Walter S, Badheka R, Trimmel G, Masse S, et al. Systematic Structural characterization of the high-temperature behavior of nearly stoichiometric silicon oxycarbide glasses. *Chem Mater* 2004;**16**:2585–98.
5. Kamiya K, Katayama A, Suzuki H, Nishida K, Hashimoto T, Matsuoka J, et al. Preparation of silicon oxycarbide glass fibers by sol–gel method—effect of starting sol composition on tensile strength of fibers. *J Sol–Gel Sci Technol* 1999;**14**:95–102.
6. Yajima S, Hayashi, Omori J, Okamura K. Development of a silicon carbide fibre with high tensile strength. *Nature* 1976;**261**:683–5.
7. Saha A, Raj R. Crystallization maps for SiCO amorphous ceramics. *J Am Ceram Soc* 2007;**90**:578–83.
8. Riedel R, Kienzle A, Dressler W, Ruwisch L, Bill J, Aldinger F. A silicoboron carbonitride ceramic stable to 2,000 degrees C. *Nature* 1996;**382**:796–8.
9. Kroke E, Li YL, Konetschny C, Lecomte E, Fasel C. Silazane derived ceramics and related materials. *Mater Sci Eng R* 2000;**26**:97–199.
10. Klonczynski A, Schneider G, Riedel R, Theissmann R. Influence of boron on the microstructure of polymer derived SiCO ceramics. *Adv Eng Mater* 2004;**6**:64–8.
11. Liebau V, Hauser R, Riedel R. Amorphous SiBCO ceramics derived from novel polymeric. *C R Chim* 2004;**7**:463–9.
12. Schiavon MA, Gervais C, Babonneau F, Soraru GD. Crystallization behavior of novel silicon boron oxycarbide glasses. *J Am Ceram Soc* 2004;**87**:203–8.
13. Peña-Alonso R, Mariotto G, Gervais C, Babonneau F, Sorarù GD. New insights on the high-temperature nanostructure evolution of SiOC and B-doped SiBOC polymer-derived glasses. *Chem Mater* 2007;**19**:5694–702.

14. Ischenko V, Pippel E, Woltersdorf J, Yappi BRN, Hauser R, Fasel C, et al. Influence of the precursor cross-linking route on the thermal stability of Si–B–C–O ceramics. *Chem Mater* 2008;**20**:7148–56.
15. Ngoumeni-Yappi R, Fasel C, Riedel R, Ischenko V, Pippel E, Woltersdorf J, et al. Tuning of the rheological properties and thermal behavior of boron-containing polysiloxanes. *Chem Mater* 2008;**20**:3601–8.
16. Sorarù GD, Dallabona N, Gervais C, Babonneau F. Organically modified SiO_2–B_2O_3 gels displaying a high content of borosiloxane (=B–O–Si$\equiv$) bonds. *Chem Mater* 1999;**11**:910–9.
17. Sorarù GD. Hybrid $RSiO_{1.5}$/B_2O_3 gels from modified silicon alkoxides and boric acid. *J Sol–Gel Sci Technol* 2000;**18**:11–9.
18. Schiavon MA, Armelin NA, Yoshida IVP. Novel poly(borosiloxane) precursors to amorphous SiBCO ceramics. *Mater Chem Phys* 2008;**112**:1047–54.
19. Peña-Alonso R, Sorarù GD. Synthesis and characterization of hybrid borosiloxane gels as precursors for Si–B–O–C fibers. *J Sol–Gel Sci Technol* 2007;**43**:313–9.
20. Bernard S, Weinmann M, Gerstel P, Miele P, Aldinger F. Boron-modified polysilazane as a novel single-source precursor for SiBCN ceramic fibers: synthesis, melt-spinning, curing and ceramic conversion. *J Mater Chem* 2005;**15**:289–99.
21. Anderson DR. In: Lee Smith A, editor. *Analysis of silicones* Wiley-Interscience: New York; 1974.
22. Peña Alonso R, Rubio F, Rubio J, Oteo JL. Characterisation of the pyrolysis process of boron-containing ormosils by FT-IR analysis. *J Anal Appl Pyrolysis* 2004;**71**:827–45.
23. Innocenzi P, Brusatin G, Guglielmi M, Bertani R. New synthetic route to (3-glycidoxypropyl)trimethoxysilane-based hybrid organic-inorganic materials. *Chem Mater* 1999;**11**:1672–9.
24. O′Shaughnessy WS, Gao M, Gleason KK. Initiated chemical vapor deposition of trivinyltrimethylcyclotrisiloxane for biomaterial coatings. *Langmuir* 2006;**22**:7021–6.
25. Peña Alonso R, Rubio J, Rubio F, Oteo JL. FT-IR and porosity study of Si–B–C–O materials obtained from TEOS–TEB–PDMS derived gel precursors. *J Sol–Gel Sci Technol* 2003;**26**:195–9.
26. Irwin AD, Holmgren JS, Zerda TW, Jonas J. Spectroscopic investigations of borosiloxane bond formation in the sol–gel process. *J Non-Cryst Solids* 1987;**89**:191–205.
27. Grill A, Neumayer DA. Structure of low dielectric constant to extreme low dielectric constant SiCOH films: Fourier transform infrared spectroscopy characterization. *J Appl Phys* 2003;**94**:6697–707.
28. Soraru GD, Babonneau F, Maurina S, Vicens J. Sol–gel synthesis of SiBOC glasses. *J Non-Cryst Solids* 1998;**224**:173–83.
29. Jenett H, Ai XT, Hodoroaba V, Iga I, Tao LM. Low-energy BO and BO_2 emission from H2BO3 sputtered in a low-pressure high-frequency SNMS plasma. *Nucl Instrum Meth B* 1999;**155**:13–24.
30. Mutin PH. Control of the composition and structure of silicon oxycarbide and oxynitride glasses derived from polysiloxane precursors. *J Sol–Gel Sci Technol* 1999;**14**:27–38.
31. Mutin PH. Role of redistribution reactions in the polymer route to silicon-carbon-oxygen ceramics. *J Am Ceram Soc* 2002;**85**:1185–9.
32. Bois L, Maquet J, Babonneau F. Structural characterization of sol–gel derived oxycarbide glasses. 1. Study of the pyrolysis process. *Chem Mater* 1994;**6**:796–802.
33. Francis A, Ionescu E, Fasel C, Riedel R. Crystallization behavior and controlling mechanism of iron-containing Si-C-N cermics. *Inorg Chem* 2009;**48**:10078–83.
34. Kasgoz A, Misono T, Abe Y. Preparation and properties of polyborosiloxanes as precursors for borosilicate formation of SiO_2–B_2O_3 gel fibers and oxides by the sol–gel method using tetraacetoxysilane and boron tri-n-butoxide. *J Polym Sci* 1994;**32**:1049–56.
35. Jacques S, Guette A, Bourrat X, Langlais F, Guimon C, Labrugere C. LCVD and characterization of boron-containing pyrocarbon materials. *Carbon* 1996;**34**:1135–43.
36. Miura Y, Kusano H, Nanba T, Matsumoto S. X-ray photoelectron spectroscopy of sodium borosilicate glasses. *J Non-Cryst Solids* 2001;**290**: 1–14.
37. Gervais C, Babonneau F, Dallabonna N, Sorarù GD. Sol–gel-derived silicon-boron oxycarbide glasses containing mixed silicon oxycarbide (SiC_xO_{4-x}) and boron oxycarbide (BC_yO_{3-y}) units. *J Am Ceram Soc* 2001;**84**:2160–4.
38. Cançado LG, Jorio A, Pinenta MA. Measuring the absolute Raman cross section of nanographites as a function of laser energy and crystallite size. *Phys Rev B* 2007;**76**:064304-1–7.
39. Ferrari AC, Robertson J. Interpretation of Raman spectra of disordered and amorphous carbon. *Phys Rev B* 2000;**61**:14095–107.
40. Pinenta MA, Dresselhaus G, Dersselhaus MS, Cançado LG, Jorio A, Saito R. Studying disorder in graphite-based systems by Raman spectroscopy. *Phys Chem Chem Phys* 2007;**9**:1276–91.
41. Ferrari AG, Meyer JC, Scardaci V, Casiraghi C, Lazzeri M, Mauri F, et al. Raman spectrum of graphene and graphene layers. *Phys Rev Lett* 2006;**97**:187401-1–4.